# Refined second-order plastic-hinge dynamic analysis for planar steel frames

IOP Conf. Series: Journal of Physics: Conf. Series **1425** (2020) 012047 doi:10.1088/1742-6596/1425/1/012047

# Refined second-order plastic-hinge dynamic analysis for planar steel frames

**Văn Tú Nguyễn, Thanh Bình Phạm, Xuân Bàng Nguyễn**
Institute of Techniques for Special Engineering, Le Quy Don Technical University, Viet Nam.

Email: nguyentu@lqdtu.edu.vn

**Abstract**. The paper presents the method of the refined second-order plastic hinge analysis for planar steel frames subjected to dynamic loads. The material model used is the generalized Clough model in consideration of effects of axial and shear force on plastic limit state of cross-sections. Geometric nonlinearities of member and frame are taken into account by the use of stability functions in framed stiffness matrix formulation. Non-linear motional equation of structures was established by finite element method and solved by Newmark method combined with the modified Newton-Raphson method. Based on the obtained algorithms, the author has programmed a computational program and calculated the planar steel frames. From the calculated results, discussions and conclusions are presented.

## 1. Introduction

In paper [17, 18, 19], the author has studied the elasto-plastic planar steel frames subjected to dynamic loads. The material model used is the generalized Clough model (see figure 1) in consideration of effects of axial and shear force on plastic limit state of cross-sections. In the second-order plastic hinge analysis, material and geometric nonlinearities are considered. In there, geometric nonlinearities of member and frame are taken into account by the use of stability functions in framed stiffness matrix formulation. This method accounts for inelasticity but not the spread of yielding through the section or between the hinges. The effect of residual stresses between hinges is not accounted for either [5,6,10,11].

In the refined second-order plastic hinge analysis, two modifications are made to account for: (1) the section stiffness degradation right at the plastic location; and (2) the member stiffness degradation between two plastic hinges. The section stiffness degradation function is used to reflect the gradual yielding through the cross section that takes place as the plastic hinge form [1, 13]. The tangent modulus concept is used to capture the residual stress effect along the member between two plastic hinges [4,21]. The material model used is the elastic–perfectly plastic [2, 10, 13, 20].

In this paper, refined second-order plastic hinge analysis for planar steel frames subjected to dynamic loads is developed. The material model used is the generalized Clough model in consideration of effects of axial and shear force on plastic limit state of cross-sections. The material nonlinearities are considered by using CRC tangent modulus and a parabolic function [21]. The

geometric nonlinearities are considered by stability function accounting for the interaction between axial force and bending moment [6, 16].

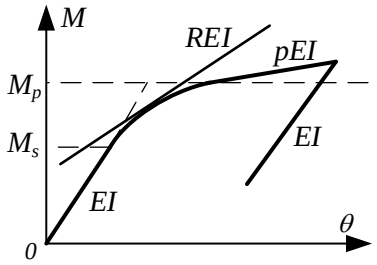


**Figure 1.** The moment–rotation curve of the generalized Clough model [18].

in figure 1: $M_p$ is the full plastic moment of cross-section; $M_s$ is the initial yielding moment; $E$ is modulus of elasticity; $p$ is the hardening factor, $I$ is the moment of internal; $R$ is the recovery force parameter [12, 17].

The assumptions used in this paper are as follow:

- All elements are initially straight and prismatic. Plane cross-sections remain plane after deformation.

- Large displacements are allowed, but strains are small. The strain reversal effect is treated by the application of double modulus theory.

- The material model used is the generalized Clough model in consideration of effects of axial and shear force on plastic limit state of cross-sections [14, 18].

- The member shear forces are smaller enough that the effects of shear deformation can be neglected.

- The element stiffness formulation is based on beam-column stability function including axial and bending deformations.

- The static load due to the weight of the mass and dead loading (if any) is applied first to the structure by a static analysis, and then the earthquake loading is applied by a dynamic time-history analysis.

- The element reamains elastic except at its ends where zero length plastic hinges form (concentrated plasticity). The beam-to-column connections of steel frame are the perfectly rigid joints.

## 2. Element stiffness matrix in local axis

### *2.1. Stability functions accounting for second-order effects*

From Kim et al., the incremental form of member basic force and deformation relationship of 2D beam–column element can be expressed as [1, 6]:

$$\begin{Bmatrix} M_A \\ M_B \\ N \end{Bmatrix} = \frac{EI}{L} \begin{bmatrix} S_1 & S_2 & 0 \\ S_2 & S_1 & 0 \\ 0 & 0 & A/I \end{bmatrix} \begin{Bmatrix} \theta_A \\ \theta_B \\ e \end{Bmatrix}. \tag{1}$$

where $M_A$, $M_B$ are the end moments at element ends $A$ and $B$; $N$ is the axial force; $L$ is the undeformed length of the element; $A$ is the area of an element cross section; $\theta_A, \theta_B$ are the joint rotations; $e$ is the axial displacement of the member; $S_1$ and $S_2$ are the stability functions, which may be written as [3, 6]:

$$S_1 = \begin{cases} \dfrac{\rho\sin\rho - \rho^2\cos\rho}{2 - 2\cos\rho - \rho\sin\rho} & if \ \ N < 0 \\ \dfrac{\rho^2\cosh\rho - \rho\sinh\rho}{2 - 2\cosh\rho + \rho\sinh\rho} & if \ \ N > 0. \end{cases} \tag{2}$$

$$S_2 = \begin{cases} \dfrac{\rho^2 - \rho\sin\rho}{2 - 2\cos\rho - \rho\sin\rho} & if\ \ N < 0 \\ \dfrac{\rho\sinh\rho - \rho^2}{2 - 2\cosh\rho + \rho\sinh\rho} & if\ \ N > 0. \end{cases} \tag{3}$$

where $\rho = L\sqrt{|N| / EI}$ và $N$ is taken as positive in tension.

$S_1$ and $S_2$ account for the effect of the axial force on the bending stiffness of the member. Equations (2) and (3) are indeterminate when the axial force is equal to zero. To circumvent this problem, the following simplified equations are used to approximate the stability function when the axial force in the member falls within the range of $-2.0 \le \rho \le 2.0$ [1, 6]:

$$S_1 = 4 + \frac{2\pi^2\rho_e}{15} - \frac{(0.01\rho_e + 0.543)\rho_e^2}{4 + \rho_e} - \frac{(0.004\rho_e + 0.285)\rho_e^2}{8.183 + \rho_e} \tag{4}$$

$$S_2 = 2 - \frac{\pi^2\rho_e}{30} + \frac{(0.01\rho_e + 0.543)\rho_e^2}{4 + \rho_e} - \frac{(0.004\rho_e + 0.285)\rho_e^2}{8.183 + \rho_e}. \tag{5}$$

where $\rho_e = N / N_e = N / \left(\pi^2 EI / L^2\right)$ , N > 0 in tension.

Equations (1) may be written as

$$\{f_e\} = [k_e]\{d_e\}. \tag{6}$$

where $\{f_e\}, \{d_e\}$ are the element force and displacement vectors, respectively, and $[k_e]$ is the element basic tangent stiffness matrix in local axis.

$$[k_e] = \frac{EI}{L}\begin{bmatrix} S_1 & S_2 & 0 \\ S_2 & S_1 & 0 \\ 0 & 0 & A/I \end{bmatrix}. \tag{7}$$

*2.2. CRC tangent modulus model associated with residual stresses*

The CRC tangent modulus concept is used to account for gradual yielding (due to residual stresses) along the length of axially loaded members between plastic hinges. The elastic modulus E (instead of moment of inertia I) is reduced to account for the reduction of the elastic portion of the cross-section since the reduction of the elastic modulus is easier to implement than a new moment of inertia for every different section. From Chen and Lui (1992), the CRC tangent modulus $E_t$ is written as [3, 21]

$$E_t = 1.0E \ for \ N \le 0.5N_y \tag{8}$$

$$E_t = \frac{4NE}{N_y}\left(1 - \frac{N}{N_y}\right) \ for \ \ N > 0.5N_y. \tag{9}$$

where $N_y$ is the yielding axial force, $N_y = \sigma_y A$.

*2.3. Parabolic function accounting for gradual yielding due to flexure*

The tangent modulus model is suitable for a member subjected to axial force, but not adequate for cases of both axial force and bending moment. A gradual stiffness degradation model for a plastic-hinge is required to represent the partial plastification effects associated with bending. When softening plastic-hinges are active at both ends of an element, the force–deflection equation may be expressed as [6]:

$$\begin{Bmatrix} M_A \\ M_B \\ N \end{Bmatrix} = \begin{bmatrix} k_{11} & k_{12} & 0 \\ k_{21} & k_{22} & 0 \\ 0 & 0 & E_t A / L \end{bmatrix} \begin{Bmatrix} \theta_A \\ \theta_B \\ e \end{Bmatrix} \tag{10}$$

where

$$k_{11} = \phi_A \left( S_1 - \frac{S_2^2}{S_1}\left[1-\phi_B\right] \right) \frac{E_t I}{L},\ k_{12} = k_{21} = \phi_A \phi_B S_2 \frac{E_t I}{L},\ k_{22} = \phi_B \left( S_1 - \frac{S_2^2}{S_1}\left[1-\phi_A\right] \right) \frac{E_t I}{L}. \tag{11}$$

The terms $\phi_A, \phi_B$ are scalar parameters that allow for gradual inelastic stiffness reduction of the element associated with plastification at ends *A* and *B*. These terms are equal to 1.0 when the element is elastic, and zero when a plastic hinge is formed. The parameter $\phi$ is assumed to vary according to the parabolic function [1, 6]:

$$\phi_i = \begin{cases} 1 & for\ \alpha_i \le 0.5 \\ 4\alpha_i \left(1-\alpha_i\right) & for\ \alpha_i > 0.5. \end{cases} \tag{12}$$

where $\alpha_i$ is a force-state parameter that measures the magnitude of axial force and bending moment at the element end. The term α in this study is expressed as [1, 6, 7]:

$$\alpha = \frac{N}{N_y} + \frac{8M}{9M_p} \quad \text{for } \frac{N}{N_y} \ge \frac{2M}{9M_p} \tag{13}$$

$$\alpha = \frac{N}{2N_y} + \frac{M}{M_p} \quad \text{for } \frac{N}{N_y} < \frac{2M}{9M_p}. \tag{14}$$

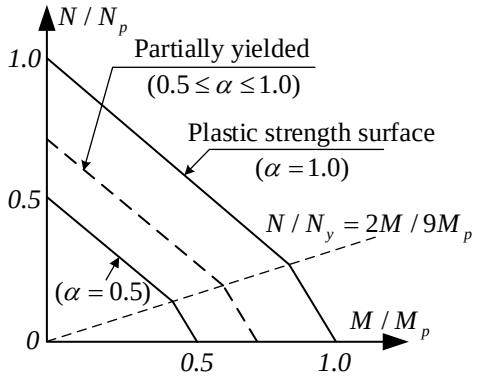


**Figure 2.** Two-surface stiffness degradation model for refined plastic hinge analysis [6, 7, 16].

To treat the strain reversal effect in the hinge due to the abrupt change in applied direction of dynamic load, the scalar parameter $\phi$, which allows for gradual inelastic stiffness reduction of the element associated with plastification at member end as presented in equation (12), is modified based on the double modulus theory in Chen and Lui (1987) as follows [3, 4]:

$$\phi_d = \frac{2\phi_s}{1+\phi_s}. \tag{15}$$

where $\phi_d$ is the scalar parameter in dynamic analysis; $\phi_s$ is the scalar parameter in static analysis determined by equation (12).

*2.4. Shear deformation*

Accounting for transverse shear deformation effects in a beam-column element, the stiffness matrix may be modified as [1, 5, 11]:

$$\begin{Bmatrix} M_A \\ M_B \\ N \end{Bmatrix} = \begin{bmatrix} c_{11} & c_{12} & 0 \\ c_{21} & c_{22} & 0 \\ 0 & 0 & E_t A / L \end{bmatrix} \begin{Bmatrix} \theta_A \\ \theta_B \\ e \end{Bmatrix} \tag{16}$$

in which

$$c_{11} = \frac{k_{11}k_{22} - k_{12}^2 + k_{11}A_s GL}{k_{11} + k_{22} + 2k_{12} + A_s GL},\ c_{12} = c_{21} = \frac{-k_{11}k_{22} + k_{12}^2 + k_{12}A_s GL}{k_{11} + k_{22} + 2k_{12} + A_s GL},\ c_{22} = \frac{k_{11}k_{22} - k_{12}^2 + k_{22}A_s GL}{k_{11} + k_{22} + 2k_{12} + A_s GL}. \tag{17}$$

where $A_s$ is the shear areas, $G$ is the shear modulus of elasticity of steel.

## 3. Element stiffness matrix in global axis

In a second-order analysis, it is convenient to express the element force displacement equations in an increment form. Denoting $\dot{M}_A, \dot{M}_B, \dot{\theta}_A, \dot{\theta}_B$ as the incremental end moments and joint rotations at element ends *A* and *B*, respectively, and $\dot{N}, \dot{e}$ as the incremental axial force and displacement in the longitudinal direction of the element, an incremental form of equation (1) may be written as [6]:

$$\begin{Bmatrix} \dot{M}_A \\ \dot{M}_B \\ \dot{N} \end{Bmatrix} = \begin{bmatrix} S_1 & S_2 & 0 \\ S_2 & S_1 & 0 \\ 0 & 0 & EA / L \end{bmatrix} \begin{Bmatrix} \dot{\theta}_A \\ \dot{\theta}_B \\ \dot{e} \end{Bmatrix} \tag{18}$$

$$\left\{ \dot{f}_e \right\} = \left[ k_e \right] \left\{ \dot{d}_e \right\}. \tag{19}$$

where $\left\{ \dot{f}_e \right\}, \left\{ \dot{d}_e \right\}$ are the incremental force and displacement vectors, respectively.

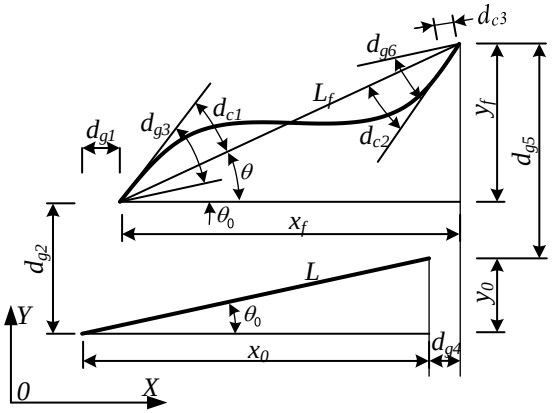


**Figure 3.** Global and local displacements of a beam-column element.

If $\left\{ d_g \right\} = \left\{ d_{g1} \quad d_{g2} \quad d_{g3} \quad d_{g4} \quad d_{g5} \quad d_{g6} \right\}^T$ are defined as the global translational and rotational degrees of freedom of a frame member (see figure 3), it can be shown that the local displacements are related to the global displacements by

$$\left\{ \dot{d}_e \right\} = \left[ T_e \right] \left\{ \dot{d}_g \right\} \tag{20}$$

where $\left[ T_e \right]$ is the element transformation matrix, may be written as

$$\left[ T_e \right] = \begin{bmatrix} -\mathrm{s}/L & c/L & 1 & s/L & -c/L & 0 \\ -s/L & c/L & 0 & s/L & -c/L & 1 \\ -c & -s & 0 & c & s & 0 \end{bmatrix} \tag{21}$$

where $c = \cos\theta; s = \sin\theta$ .

Based on the principle of equilibrium, the forces in the two systems shown in figure 4 are related by

$$\left\{ f_g \right\} = \left[ T_e \right]^T \left\{ f_e \right\} \tag{22}$$

where $\left\{ f_g \right\} = \left\{ f_{g1} \quad f_{g2} \quad f_{g3} \quad f_{g4} \quad f_{g5} \quad f_{g6} \right\}^T$, $\left\{ f_e \right\} = \left\{ M_A \quad M_B \quad N \right\}^T$ are the force vectors in the global and local axis, respectively, shown in figure 4.

Taking derivatives on both sides of equation (22) gives

$$\left\{ \dot{f}_g \right\} = \left[ \dot{T}_e \right]^T \left\{ f_e \right\} + \left[ T_e \right]^T \left\{ \dot{f}_e \right\} \tag{23}$$

In view of equation (18) and (20), equation (23) may be further written as

$$\left\{ \dot{f}_g \right\} = \left[ \dot{T}_e \right]^T \left\{ f_e \right\} + \left[ T_e \right]^T \left[ k_e \right] \left[ T_e \right] \left\{ \dot{d}_g \right\} \tag{24}$$

The transformation matrix $\left[ \dot{T}_e \right]^T$ can be evaluated by taking the derivative of $\left[ T_e \right]$ with respect to each global degree of freedom, $d_{gi}$ as

$$\left[ \dot{T}_e \right]^T = \left[ \frac{\partial \left[ T_e \right]^T}{\partial d_{gi}} \right] \left\{ \dot{d}_{gi} \right\}, i = 1 \div 6 \tag{25}$$

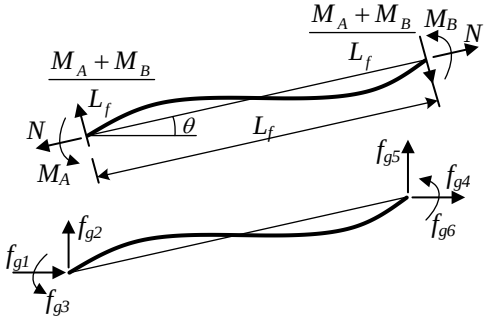


**Figure 4.** Equivalent force system.

In view of equation (20), equation (25) may be written as

$$\left[ \dot{T}_e \right]^T = \left[ \frac{\partial^2 d_{ek}}{\partial d_{gj} \partial d_{gi}} \right]^T \left\{ \dot{d}_{gi} \right\}; i, j = 1 \div 6; k = 1 \div 3 \tag{26}$$

or

$$\left[ \dot{T}_e \right]^T = \left[ \frac{\partial^2 d_{e1}}{\partial d_{gj} \partial d_{gi}} \middle| \frac{\partial^2 d_{e3}}{\partial d_{gj} \partial d_{gi}} \middle| \frac{\partial^2 d_{e3}}{\partial d_{gj} \partial d_{gi}} \right]^T \left\{ \dot{d}_{gi} \right\} = \left[ \left[ T_1 \right] \middle| \left[ T_2 \right] \middle| \left[ T_3 \right] \right] \left\{ \dot{d}_{gi} \right\} \tag{27}$$

where

$$\left[ T_1 \right] = \left[ T_2 \right] = \frac{1}{L^2} \begin{bmatrix} -2sc & c^2 - s^2 & 0 & 2sc & s^2 - c^2 & 0 \\ c^2 - s^2 & 2sc & 0 & s^2 - c^2 & -2sc & 0 \\ 0 & 0 & 0 & 0 & 0 & 0 \\ 2sc & s^2 - c^2 & 0 & -2sc & c^2 - s^2 & 0 \\ s^2 - c^2 & -2sc & 0 & c^2 - s^2 & 2sc & 0 \\ 0 & 0 & 0 & 0 & 0 & 0 \end{bmatrix} \tag{28}$$

$$\left[T_3\right]=\frac{1}{L}\begin{bmatrix} s^2 & -sc & 0 & -s^2 & sc & 0 \\ -sc & c^2 & 0 & sc & -c^2 & 0 \\ 0 & 0 & 0 & 0 & 0 & 0 \\ -s^2 & sc & 0 & s^2 & -sc & 0 \\ sc & -c^2 & 0 & -sc & c^2 & 0 \\ 0 & 0 & 0 & 0 & 0 & 0 \end{bmatrix} \tag{29}$$

Substituting Equation (27) into Equation (24) gives

$$\left\{\dot{f}_g\right\}=\left[k_g\right]\left\{\dot{d}_g\right\} \tag{30}$$

where $\left[k_g\right]$ is the tangent stiffness matrix of the beam-column element in global axis, are given as

$$\left[k_g\right]=\left[T_e\right]^T\left[k_e\right]\left[T_e\right]+\left[T_1\right]M_A+\left[T_2\right]M_B+\left[T_3\right]N \tag{31}$$

Equation (31) represents the element tangent stiffness matrix in global axis when the element is elastic ($\phi=1$). When a plastic hinge is formed at end *A* or *B*, stiffness matrix $\left[k_e\right]$ is replaced with the matrixs $\left[k_A\right],\left[k_B\right],\left[k_{AB}\right]$, equation (31) is revised as

When the plastic hinge is formed at end *A*:

$$\left[k_{gpA}\right]=\left[T_e\right]^T\left[k_A\right]\left[T_e\right]+\left[T_1\right]M_A+\left[T_2\right]M_B+\left[T_3\right]N\,, \tag{32}$$

When the plastic hinge is formed at end *B*:

$$\left[k_{gpB}\right]=\left[T_e\right]^T\left[k_B\right]\left[T_e\right]+\left[T_1\right]M_A+\left[T_2\right]M_B+\left[T_3\right]N\,, \tag{33}$$

And when the plastic hinge is formed at end *A* and *B*:

$$\left[k_{gpAB}\right]=\left[T_e\right]^T\left[k_{AB}\right]\left[T_e\right]+\left[T_1\right]M_A+\left[T_2\right]M_B+\left[T_3\right]N\,. \tag{34}$$

The stiffness matrixs determined according to equations (32-34) are based on the assumption of the material model used is elastic–perfectly plastic. When the material model used is the generalized Clough model, the element matrixs in global may be expressed as

$$\left[k_{gC}\right]=R_B\left[k_g\right]+\left(\mathrm{R}_A-\mathrm{R}_B\right)\left[k_{gpB}\right]+\left(1-\mathrm{R}_A\right)\left[k_{gpAB}\right],\ \text{when}\ R_A\ge R_B, \tag{35}$$

$$\left[k_{gC}\right]=R_A\left[k_g\right]+\left(\mathrm{R}_B-\mathrm{R}_A\right)\left[k_{gpA}\right]+\left(1-\mathrm{R}_B\right)\left[k_{gpAB}\right],\ \text{when}\ R_B\ge R_A, \tag{36}$$

where $R_A$ and $R_B$ are the recovery force parameters for end *A* and end *B* of the element, respectively, which are relevant to the moments at the both ends of the element, $M_A$ and $M_B$, and the deformation state of the element, and may be expressed as [12, 17]:

- if $M < M_s$ then R = 1; (37)
- if $M > M_p$ then R = p; (38)
- if $M_s < M < M_p$ then $R=1-\dfrac{M-M_s}{M_p-M_s}\left(1-p\right)$. (39)

## 4. The equation of motion and solving method

The equation of motion for frames is given by [8, 9]:

$$\left[M\left(\{U\}\right)\right]\left\{\ddot{U}\right\}+\left[C\left(\{U\}\right)\right]\left\{\dot{U}\right\}+\left[K\left(\{U\}\right)\right]\{U\}=\{R\} \tag{40}$$

where $\{U\},\{\dot{U}\},\{\ddot{U}\},\{R\}$ are the structural displacement, velocity, acceleration, and exciting force vectors, respectively; $\left[M\left(\{U\}\right)\right]$ is the structural mass matrix; the structural viscous damping matrix $\left[C\left(\{U\}\right)\right]$ can be defined as Rayleigh damping, $\left[C\left(\{U\}\right)\right]=\gamma\left[M\left(\{U\}\right)\right]+\beta\left[K\left(\{U\}\right)\right]$, where $\gamma$ and $\beta$ are the coefficients of mass and stiffness proportional damping, respectively and are determined according to the natural frequencies of the first and second modes of the frame $\omega_1,\omega_2$ and the same viscous damping ratio $\zeta=5\%$; $\left[K\left(\{U\}\right)\right]$ is the structural stiffness matrix.

Equation (40) is the nonlinear differential equation for the displacement vector $\{U\}$. To solve this equation, we use the Newmark average acceleration method combined with the modified Newton-Raghson method for the equilibrium iterative procedure.

Divide the analysis time into intervals $\Delta t$, the Newmark algorithm written at $t+\Delta t$ will lead equation (40) to form [9, 15]:

$$\left[\hat{K}_t\right]\{\Delta U\}=\left\{\Delta\hat{R}\right\}_{t+\Delta t}, \tag{41}$$

where

$$\{\Delta U\}=\{U\}_{t+\Delta t}-\{U\}_t,\left[\hat{K}_t\right]=\left[K_t\right]+\frac{\delta}{\alpha\Delta t}\left[C_t\right]+\frac{1}{\alpha\left(\Delta t\right)^2}\left[M_t\right], \tag{42}$$

$$\left\{\Delta\hat{R}\right\}_{t+\Delta t}=\{R\}_{t+\Delta t}-\{R\}_t+\left(\frac{1}{\alpha\Delta t}\left[M_t\right]+\frac{\delta}{\alpha}\left[C_t\right]\right)\left\{\dot{U}\right\}_t+\left[\frac{1}{2\alpha}\left[M_t\right]+\Delta t\left(\frac{\delta}{2\alpha}-1\right)\left[C_t\right]\right]\left\{\ddot{U}\right\}_t. \tag{43}$$

where $\left[M_t\right],\left[C_t\right]$ are the structural mass and damping matrix at the time *t*, respectively. These are formed from the element matrixs deformed according to the generalized Clough model and are defined in [17]. $\left[K_t\right]$ is the structural stiffness matrix at the time *t* and is determined from the element stiffness matrix in global axis defined in section 3. $\left\{\dot{U}\right\}_t,\left\{\ddot{U}\right\}_t$ are the structural velocity, acceleration vectors at the time *i*, respectively.

The incremental displacement vector $\{\Delta U\}$ at the time $t+\Delta t$, can be calculated from Equation (41), from that determined $\{U\}_{t+\Delta t},\left\{\dot{U}\right\}_{t+\Delta t}\left\{\ddot{U}\right\}_{t+\Delta t}$ as follows [8,15]:

$$\left\{\Delta\dot{U}\right\}=\frac{\delta}{\alpha\Delta t}\{\Delta U\}-\frac{\delta}{\alpha}\left\{\dot{U}\right\}_t+\Delta t\left(1-\frac{\delta}{2\alpha}\right)\left\{\ddot{U}\right\}_t, \tag{44}$$

$$\left\{\Delta\ddot{U}\right\}=\frac{1}{\alpha\left(\Delta t\right)^2}\{\Delta U\}-\frac{1}{\alpha\Delta t}\left\{\dot{U}\right\}_t-\frac{1}{2\alpha}\left\{\ddot{U}\right\}_t, \tag{45}$$

$$\begin{aligned}&\{U\}_{t+\Delta t}=\{U\}_t+\{\Delta U\};\left\{\dot{U}\right\}_{t+\Delta t}=\left\{\dot{U}\right\}_t+\left\{\Delta\dot{U}\right\};\\&\left\{\ddot{U}\right\}_{t+\Delta t}=\left\{\ddot{U}\right\}_t+\left\{\Delta\ddot{U}\right\}.\end{aligned} \tag{46}$$

where $\alpha$ và $\delta$ are the integral parameters.

After each calculation step, it is necessary to check the internal force-displacement state $\left(M-\theta\right)$, the displacement at the element end to update the stiffness, mass, damping matrixs and force vector of the elements, and moment $M_s$, $M_p$ at the element ends to calculate the next time step. Checking is based on the relations between $R_i$ and $R_j$ [17]. The procedure presented in equations (41-46) is repeated for the next time steps until the considered frame is collapsed or desired time duration ends.

A computer program SODAP written in Matlab programming language is developed based on the above-mentioned formulations to predict nonlinear time-history responses of the planar steel frames subjected to static and dynamic loadings. The material model used is the generalized Clough model in consideration of effects of axial and shear force on plastic limit state of cross-sections.

## 5. Numerical examples and discussions

The dynamic behaviour of steel frame (see figure 5) with the generalized Clough material model is examined under seimic load. The effect of second order is also investigated with the internal force-displacement results.

The data of frame is: I-shape beam with ($hxbxt_wxt_f$ = 200x100x5.5x8 *mm*), I-shape column with section (250x125x6x8 *mm*) (see figure 5); module $E$=2.0e+5 *MPa*; yielding stress $\sigma_p$=210 *MPa; p=0.02*. The finite element diagram of structure is shown in figure 5. The frame is subjected to seismic action at Morgan Hill, 1984, in the Santa Clara Valley of Northern California with acceleration diagram measured at station 1567, direction $0^0$ as in figure 6. The peak of acceleration background is 0.292g, interval of measurement 0.005 (sec). Damping coefficient $\xi_1 = \xi_2 = 0.05$. Mass $m_1$=3.0 kN.s$^2$/m; $m_2$=1.0 kN.s$^2$/m, acceleration of gravity $g$ = 9.81 *m/s*$^2$. Dead load P=50kN.

The calculated results are shown in figure 7-11 and table 1 and 2. Figure 7 shows the diagram of horizontal displacements at node 11; figure 8 demonstrates the dynamic bending moment at node 1; figure 9 shows bending moment-rotation relationship at node 9 (in element 8) for these cases: case (a) – second-order plastic hinge analysis (*SO*); case (b) – refined second-order plastic hinge analysis (*RSO*). In figure 10 the displacement diagram, first plastic hinge location is demonstrated. The displacement diagram and locations of plastic hinges at the moment with maximum number of these hinges for cases (a) and (b) are shown in figure 11. In table 1 and table 2, the maximum and minimum displacements, bending moments at sections according to two cases analysis are detailed and compared with case (a).

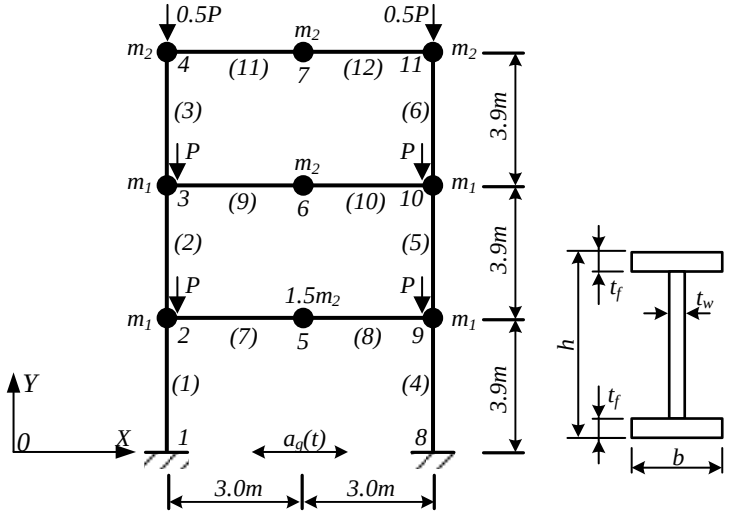


**Figure 5.** Three-storey planar steel frame for refined second-order effect verification.

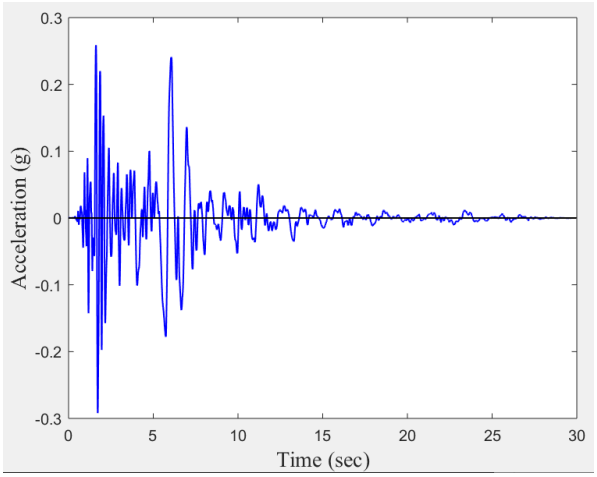


**Figure 6.** Morgan Hill, 1984, Earthquake records, Northern California, at station 1567, direction $0^0$.

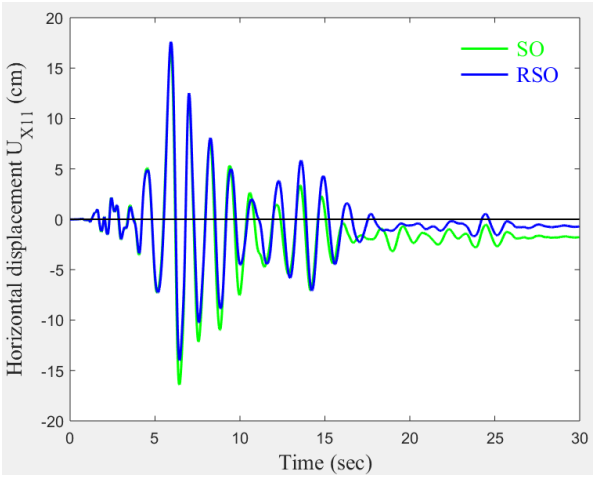


**Figure 7.** Horizontal dynamic displacement diagram at node 11.

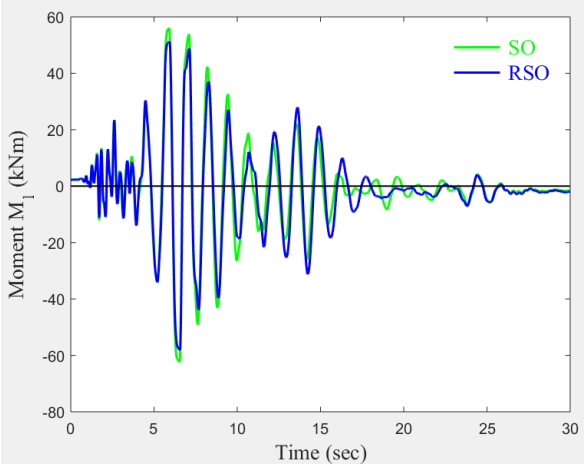


**Figure 8.** Dynamic bending moment at node 1.

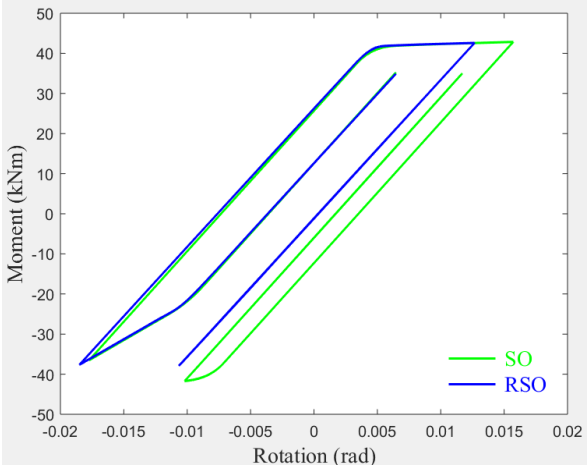


**Figure 9.** Bending moment-rotation relationship at node 9 (in element 8).

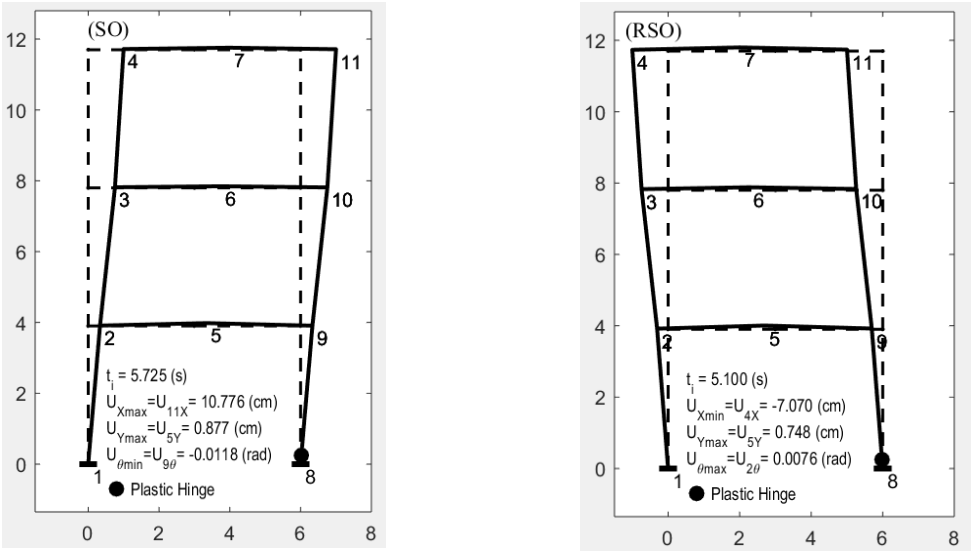


**Figure 10.** Displacement diagram and location of first plastic hinge.

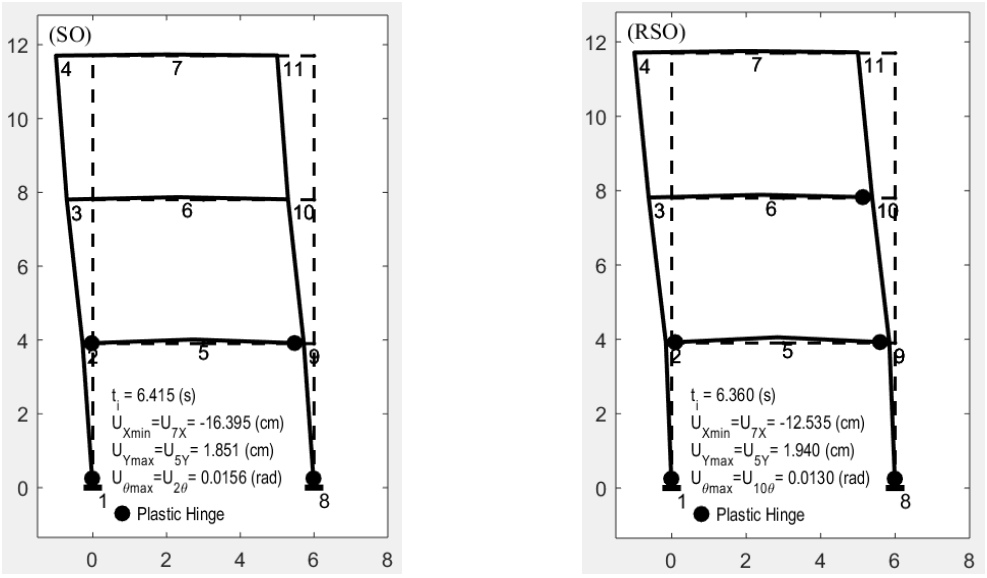


**Figure 11.** Displacement diagram and locations of plastic hinges at the moment with maximum number of plastic hinges.

**Table 1.** Maximum horizontal displacement of node 2, 3, 4.

| **Node** | | *SO* | | *RSO* | | *Ratio (1)/(3) (%)* |
|---|---|---|---|---|---|---|
| | | *Ux (cm) (1)* | *ti (s) (2)* | *Ux (cm) (3)* | *ti (s) (4)* | |
| **2** | **max** | 5.980 | 5.915 | 6.682 | 5.940 | 11.736 |
| | **min** | -6.024 | 6.535 | -5.197 | 6.555 | -13.732 |
| **3** | **max** | 12.815 | 5.920 | 13.710 | 5.940 | 6.983 |
| | **min** | -12.119 | 6.490 | -10.169 | 6.510 | -16.086 |
| **4** | **max** | 16.726 | 5.925 | 17.601 | 5.940 | 5.236 |
| | **min** | -16.427 | 6.430 | -14.009 | 6.440 | -14.719 |

**Table 2.** Maximum and minimum bending moments at some sections.

| **Node/ element** | | *SO* | | *RSO* | | *Ratio (1)/(3) (%)* |
|---|---|---|---|---|---|---|
| | | *M (kNm) (1)* | *$t_i$ (s) (2)* | *M (kNm) (3)* | *ti (s) (4)* | |
| **1/1** | **max** | 56.002 | 5.915 | 51.225 | 5.940 | -8.530 |
| | **min** | -62.347 | 6.540 | -58.141 | 6.560 | -6.747 |
| **2/2** | **max** | 43.932 | 6.960 | 42.716 | 6.985 | -2.769 |
| | **min** | -38.746 | 6.335 | -40.815 | 6.355 | 5.340 |
| **3/3** | **max** | 17.485 | 1.995 | 16.760 | 2.000 | -4.144 |
| | **min** | -10.572 | 1.865 | -9.967 | 1.870 | -5.719 |

## 6. Conclusions

When performing second-order plastic hinge dynamic analysis for planar steel frame with generalized Clough model considering the effect of axial and shear forces to limit state of cross sections, the maximum displacement will be increased (see figure 7, 9 and table 1) by 11.736% (at node 2), 5.236% (at node 4) compared to those with *SO* analysis. The reason of this increasement is the consideration of the residual displacements and gradual yielding due to flexure and shear deformation effect.

With *RSO* analysis, the maximum internal forces will be decreased. The results are shown in figure 8 and table 2. At the same time, the plastic hinges appear earlier and more than those when using *RO*

analysis (see figure 10, 11). In the figure 9, the bending moment-rotation relationship has a similar shape to the moment–rotation curve of the generalized Clough model. Therefore, the calculation results of *SODAP* ensure reliability.

Therefore, when analyzing the dynamics of planar steel frame structure, it is necessary to analyze according to refined second-order due to significant influence on displacement-internal force state of system.

**References**

[1] Chan S L and Chui P T 1999 *Non-linear static and cyclic analysis of steel frames with semi-rigid connections* (Elsevier).
[2] Chan S L 2000 Non-Linear Behavior and Design of Steel Structures *Journal of Constructional Steel Research* **57** 1217–31.
[3] Chen W F and Lui E M 1992 *Stability design of steel frames* (Boca Raton, FL: CRC Press).
[4] Chen W F and Lui E M 1987 *Structural stability: theory and implementation* (Elsevier, New York).
[5] Chen W F 2001 Practical second-order inelastic analysis for three dimensional steel frames *Steel Structures* **1(3)** 213–223.
[6] Chen W F and Sohal I 2013 *Plastic design and second-order analysis of steel frames* (Springer)
[7] Chen W F and Kim S E 1997 *LRFD steel design using advanced analysis* **13** (CRC press).
[8] Cheng F Y 2017 *Matrix analysis of structural dynamics: applications and earthquake engineering* (CRC Press).
[9] Chopra A K 2017 *Dynamics of structures. theory and applications to earthquake engineering* (Hoboken, NJ: Pearson).
[10] Davies J M 2002 Second-order elastic-plastic analysis of plane frames *J constr steel res* **58(10)** 1315–30.
[11] Kim S E 2006 Second-order inelastic dynamic analysis of 3-D steel frames *Int. J. Solids Struct.* **43(6)** 1693–1709.
[12] Li G Q and Li J J 2007 *Advanced analysis and design of steel frames* Wiley Online Library.
[13] Liew J R, White D W and Chen W F 1993 Second-order refined plastic-hinge analysis for frame design *Journal of Structural Engineering* **119(11)** 3196–3216.
[14] Neal B G 1961 The effect of shear and normal forces on the fully plastic moment of a beam of rectangular cross section *Journal of Applied Mechanics* **28(2)** 269–274.
[15] Newmark N M 1959 A method of computation for structural dynamic *J Eng Mech Div-ASCE* **85** 67–94.
[16] Orbison J G, McGuire W and Abel J F 1982 Yield surface applications in nonlinear steel frame analysis *Comput Methods Appl Mech Eng* **33** 557–73.
[17] Nguyen V T 2016 Dynamic Caculation of Elasto-plastic Planar Frame According to Generalized Clough Model *Journal of Science and Technology/Le Quy Don Technical University* **179-10** 87–93.
[18] Nguyen V T 2019 Dynamic Calculation of Elasto-plastic Planar steel Frame According to Generalized Clough Model in Consideration of Effects of Axial and Shear Force on Plastic Limit State of Cross – Sections *Vietnam Journal of Construction* **06** 117–121.
[19] Nguyen V T 2019 Second-Order Plastic-Hinge Dynamic Analysis for planar steel frames *Vietnam Journal of Construction* **09** 127–132.
[20] White D W 1993 Plastic-hinge methods for advanced analysis of steel frames *J. Constr. Steel Res* **24** 121–152.
[21] Ziemian R D and McGuire W 2002 Modified tangent modulus approach, a contribution to plastic hinge analysis *J Struct Eng ASCE* **128** 1301–07.